



Journal of Geophysical Research: Oceans

Supporting Information for

**Observed variability of the North Atlantic Current in the
Rockall Trough from four years of mooring measurements**

**L. Houpert¹, S. Cunningham², N. Fraser², C. Johnson², N. P. Holliday¹, S. Jones²,
B. Moat¹, D. Rayner¹**

¹National Oceanography Centre, Southampton, UK

²Scottish Association for Marine Science, Oban, UK

Contents of this file

Text S1 to S2

Tables S1 to S2

Figures S1 to S8

Introduction

The files included in the supplementary materials are additional text, figures and tables supporting the analysis presented in the article.

21 **Text S1: Accuracy of the mooring transport**

22

23 The details of the errors associated with the calculation of the mid-basin, western
24 wedge and eastern wedge transport are detailed below.

25

26 1 Mid-basin

27 In the mid-basin the principal sources of error are methodological (vertical and
28 surface extrapolation) and instrumental.

29 *1.1 Methodological: Vertical gridding (200m-1800m)*

30 For the mid-basin geostrophic transport calculation, temperature and salinity data
31 at the Eastern and Western boundaries are linearly interpolated onto a 20 dbar vertical
32 grid from the shallowest (50-100 m) to deepest measurement (1760 m). We assess the
33 gridding errors by subsampling lowered CTD profiles from 28 EEL hydrographic
34 sections [\(1978-2018\)](#) at the location and depths of the moored instruments. These sub-
35 sampled profiles are then vertically gridded as for the mooring data and used to
36 compute the geostrophic transport. The latter is then compared to the geostrophic
37 transport value computed from the full CTD profile. For a complete moored data return,
38 such as in 2015-2016 and 2017-2018, the RMS error is ~ 0.30 Sv and the mean bias
39 error ~ 0.10 Sv. Some data losses occurred in other periods resulting in higher RMS
40 and bias errors (Table S1, Figure S5).

41

42 *1.2 Methodological: Surface extrapolation (10-200m)*

43 The mooring designs have the shallowest measurement at 50 m (100 m before
44 2017). Therefore, data have to be extrapolated to the surface so that transports can be
45 calculated over the full water column. A number of approaches exist. At the RAPID
46 array, a seasonally-varying climatology is used to determine the vertical gradients of
47 temperature and salinity, with these being used to aid extrapolation of the shallowest
48 temperature and salinity data to the surface (McCarthy et al., 2015). As winter
49 convection in the Rockall Trough can reach 600 m (Holliday et al. 2000) and is spatially

50 and temporally variable, monthly climatologies may not adequately constrain the
51 surface extrapolation. Therefore, we take a simple approach of replicating the
52 shallowest values of temperature and salinity to the surface maintaining a constant
53 geostrophic shear.

54 The vast majority of the profiles have their shallowest measurements in the 50-
55 200 m range (99.7% for WB1 and 100% for EB1). Strong currents occasionally knock
56 down the moorings with the shallowest instrument being subducted. The deepest
57 events are 233 m at WB1 (September 2015) and 197 m at EB1 (March 2015).

58 Because the time-varying upper ocean stratification combines with a time-varying
59 shallowest measurement depth, the error in extrapolating the geostrophic shear to the
60 surface also has a time-dependence. To quantify this, we use temperature and salinity
61 profiles extracted at each mooring location from the Monthly Isopycnal / Mixed-layer
62 Ocean Climatology, MIMOC (Schmidtko et al., 2013). These profiles were subsampled
63 at the moored instrument depths and the shallowest temperatures and salinities copied
64 to the surface. The RMS and bias errors over the upper 200 m were computed from the
65 difference of the full and subsampled profiles. To simulate a broader range of variability
66 from the climatology, we repeated this at each mooring data time step by interpolating
67 the monthly climatological profiles on a time vector ranging from -14 to +14 days. Thus,
68 at each mooring timestamp we have 29 samples of the climatology, using the depth of
69 the shallowest instrument at that time, which are used to calculate the mean bias error
70 and the RMS error.

71 The mean bias error associated with the surface extrapolation is typically less
72 than 0.1 Sv ([Table S1](#)). However, between July 2016 and December 2016, this
73 increases to 0.22 Sv due to data loss at 250m. The RMS errors are generally small (<
74 0.03 Sv), but can increase up to 0.1 Sv during the period of data loss.

75
76
77

78

79

80 *1.3 Instrumental: Measurement accuracy*

81 The accuracy of the moored CTD data are estimated to be 1 dbar, 0.002°C and
82 0.003 in salinity over the duration of a two-year deployment (McCarthy et al., 2015;
83 <https://www.bodc.ac.uk/data/documents/nodb/pdf/37smbrochurejul08.pdf>). Using a
84 Monte Carlo approach, we found that both the pressure accuracy and the temperature
85 accuracy lead to a RMS error on transport of 0.01 Sv, while salinity accuracy leads to a
86 RMS error of 0.05 Sv. The combined effect of the pressure, temperature and salinity
87 accuracies leads to a RMS error of 0.05 Sv. The method is detailed below.

88 For each moored CTD timeseries from the WB and EB moorings, we created an
89 ensemble of 100 members with randomly perturbed pressure, temperature and salinity
90 values. We added to the original timeseries a random error taken from a normal
91 distribution. Because all the moored CTDs are calibrated against the ship-based CTD at
92 the beginning and at the end of the deployment, we do not expect any mean bias
93 between the moored CTDs and therefore the mean of the normal distribution is set to
94 zero for all instruments. We use the assumption that 99.7% of the normally distributed
95 error values lie within two times the moored CTD accuracy. Therefore, the standard
96 deviation of our normal distribution is defined as the moored CTD accuracy divided by
97 three. Then, the mid-basin geostrophic transport is calculated for every ensemble
98 member and the RMS error is estimated as the standard deviation between the 100
99 ensemble members.

100

101 2 Western wedge

102 In the western wedge the principal sources of error are methodological
103 (horizontal interpolation) and instrumental.

104 *2.1 Methodological: Horizontal interpolation*

105 Cross-section velocities at EEL station E (calculated from 12 LADCP profiles
106 acquired between 1996 and 2018) show a remarkably similar mean and standard
107 deviation compared to the four years of WB1 current-meter measurements (Figure S6).
108 The errors of our method for the western wedge transport calculation were calculated by

109 using data from the EEL LADCP cruises that sampled stations C to F in the Western
110 Rockall Trough. For each cruise, we calculated the western wedge transport following
111 two methods: using the full resolution LADCP velocity field from stations C to F, and
112 using the LADCP profile obtained at station E but extrapolated to cover the entire
113 western wedge area, following the method used to calculate the western wedge
114 mooring transport (see section 3.3),

115 We found a mean difference between the two methods (mean bias error) of -
116 0.30 Sv and a standard deviation of the difference (RMS error) of 0.62 Sv (Figure S7).

117

118 *2.2 Instrumental: Measurement accuracy*

119 The accuracy of the moored current meter is $\pm 1\%$ of the measured
120 value $\pm 0.5\text{cm/s}$

121 (https://www.bodc.ac.uk/data/documents/nodb/pdf/datasheet_aquadop_6000m.pdf).

122 Applying these values to our data results in a maximum transport error of ± 0.24 Sv. We
123 consider this to be effectively 95% of the normally distributed values; thus to compare
124 with our other RMS errors, we divide by 1.96 to obtain the 68% confidence interval
125 giving an error of ± 0.12 Sv.

126

127 3 Eastern wedge

128 In the eastern wedge the principal source of error is due to the repeated losses of
129 ADCP1 and the use of the GLORYS12v1 ocean reanalysis to create velocity time-series
130 at the location ADCP1.

131 The eastern wedge transport errors are calculated using the data from the EEL
132 LADCP cruises which sampled the eastern wedge. We calculated the error in the upper
133 750 m by comparing the “full” LADCP velocity field from the LADCP stations O, P, Q1
134 and Q to the velocity field reconstructed following the same method used for the
135 calculation of the eastern wedge mooring transport (see section 3.4). The reconstruction
136 of the velocity field from EEL data is achieved through three steps: 1) EEL-LADCP
137 cruises are used to create a profile of meridional velocity at the location of EB1 by

138 interpolating the LADCP velocity field; 2) GLORYS12 reanalysis is used to create a
139 profile of meridional velocity at the location of ADCP1 adjusted by + 7.6cm/s so the
140 2014-2015 GLORYS mean velocity at ADCP1 is the same as the observed one from
141 the recovered ADCP1; 3) The eastern wedge velocity field is created by linearly
142 interpolating the velocity between 9.6°W and 9.3°W and by linearly decreasing them to
143 zero at the edge of the continental shelf (9.2°W). We found a mean bias error in our
144 method of -0.27 Sv and a RMS error of 0.58 Sv (Figure S8).

145 Transport errors below 750 m are calculated by comparing the “full” LADCP
146 velocity field from the LADCP stations O and P with the reconstructed velocity field
147 (calculated by copying over the velocity interpolated at EB1 into the eastern wedge). We
148 found a mean bias error in our method of -0.06 Sv and a RMS error of 0.10 Sv.

149

150
151
152
153
154
155
156
157
158
159
160
161
162
163
164
165
166
167
168
169
170
171

Text S2: Comparison of near-surface current-meters and absolute surface geostrophic currents from altimetry

The surface absolute geostrophic currents from altimetry (mean and standard deviation) for the 2014-2018 period are indicated in Figure 3 (horizontal purple bars) and Table S2. Surface absolute currents have been extracted at WB1 and EB1 locations from the reprocessed global ocean gridded L4 COPERNICUS dataset. The mid-basin surface absolute geostrophic current is calculated from Absolute Dynamic Topography extracted at the locations of WB1 and EB1.

In the mid-basin, the mean and variability of the surface altimetry meridional current matches the near-surface geostrophic velocity (Figure 3). In the Western and Eastern part of the Rockall Trough, the mean absolute surface geostrophic currents from altimetry are lower than the near-surface current meter data. The differences are substantial: 4.6 cm/s at EB1 and -7.4 cm/s at WB1 (Table S2). In addition, the variability of the currents observed in situ is not well captured in the surface altimetry, indicated by the standard deviation of the surface altimetry data being only 52% of the standard deviation of the current observed in situ at WB1. Thus mismatch between in situ observation and satellite altimetry in the basin's boundary currents is consistent with the results of Pujol et al. (2016). They showed that nearly 60% of the energy observed in along-track measurements at wavelengths ranging from 200 to 65 km is missing in the Sea Level Anomaly gridded products.

172 **Table S1:** Summary of the errors for each component of the Rockall Trough transport.
173 The bias error and RMS error estimated for the western wedge (WW) and eastern
174 wedge (EW) transports are similar for all deployment periods. The western wedge
175 transport errors are due to the horizontal extrapolation of the current meters and
176 accuracy of the measurements. The eastern wedge errors are due to the horizontal
177 extrapolation and the use of an ocean reanalysis profile at the location of the ADCP
178 mooring. The mid-basin transport errors are due to the vertical gridding, the surface
179 extrapolation and the accuracy of the measurements. The higher mean bias error and
180 RMS error found in 2014-2015 are due to the failure of the the CTD deployed at 1000m
181 on EB1. The loss of the CTD deployed at 250m on EB1 in March 2017 explains the
182 higher errors found between July 2016 and May 2017. Two other events occurred
183 during that third deployment which changed the array configuration: 1) in December
184 2016, the CTD deployed at 100m on EB1 slid the wire down to 240m but continued
185 working correctly; 2) in March 2017, the top 400m of the EB1 mooring broke, certainly
186 due to fishing activities. The upper CTD and current meter were recovered on the shore
187 of St Kilda by a local boat and we were able to use the data prior to the breaking of the
188 line. However, from March 2017 to May 2017, we reconstructed the temperature and
189 salinity at 100m depth on EB1 using linear regressions with the temperature and salinity
190 timeseries from the WB1 CTD located at 100m depth (correlation coefficients of 0.93 for
191 temperature and 0.85 for salinity over the 2014-2016). The surface extrapolation error
192 on the mid-basin transport calculation has a significant time-varying component (Figure
193 S5) therefore we also indicate the minimum and maximum of the bias error for each
194 deployment.

	Jul14 - Jul18	
	Bias (Sv)	RMS (Sv)
Total WW	-0.30	0.63
Total EW	0.21	0.59

		Jul 14 – Jun 15		Jun 15 – Jul 16		Jul 16- Dec 16		Dec 16–Mar17		Mar 17–May17		May 17 – Jul 18	
		bias (Sv)	RMS (Sv)	bias (Sv)	RMS (Sv)	bias (Sv)	RMS (Sv)	bias (Sv)	RMS (Sv)	bias (Sv)	RMS (Sv)	bias (Sv)	RMS (Sv)
mid-basin	Gridding	-0.25	0.65	0.10	0.27	0.19	0.28	-0.02	0.31	0.28	0.28	0.12	0.28
	Surface extrap. * [min; max]	-0.05 [-0.09; 0.05]	0.01 [0.00; 0.03]	0.02 [-0.09; 0.17]	0.01 [0.00; 0.03]	0.22 [0.08; 0.35]	0.03 [0.00; 0.10]	-0.01 [-0.11; 0.06]	0.02 [0.00; 0.07]	0.19 [0.16; 0.22]	0.01 [-0.01; 0.01]	-0.01 [-0.07; 0.08]	0.01 [0.00; 0.03]
	Instrument accuracy	0	0.05	0	0.05	0	0.05	0	0.05	0	0.05	0	0.05
	Tot. mid-basin * [min; max]	-0.30 [-0.33; -0.19]	0.68 [0.68; 0.68]	0.11 [0.02; 0.27]	0.34 [0.33; 0.33]	0.41 [0.27; 0.55]	0.34 [0.33; 0.34]	-0.03 [-0.13; 0.04]	0.36 [0.36; 0.37]	0.47 [0.44; 0.50]	0.34 [0.34; 0.34]	0.11 [0.05; 0.20]	0.33 [0.33; 0.34]
Total Rockall Trough [min; max]	-0.39 [-0.43; -0.29]	1.10	0.03 [-0.07; 0.19]	0.93	0.32 [0.18; 0.46]	0.93	-0.12 [-0.22; -0.05]	0.94	0.38 [0.34; 0.41]	0.93	0.03 [-0.03; 0.11]	0.93	

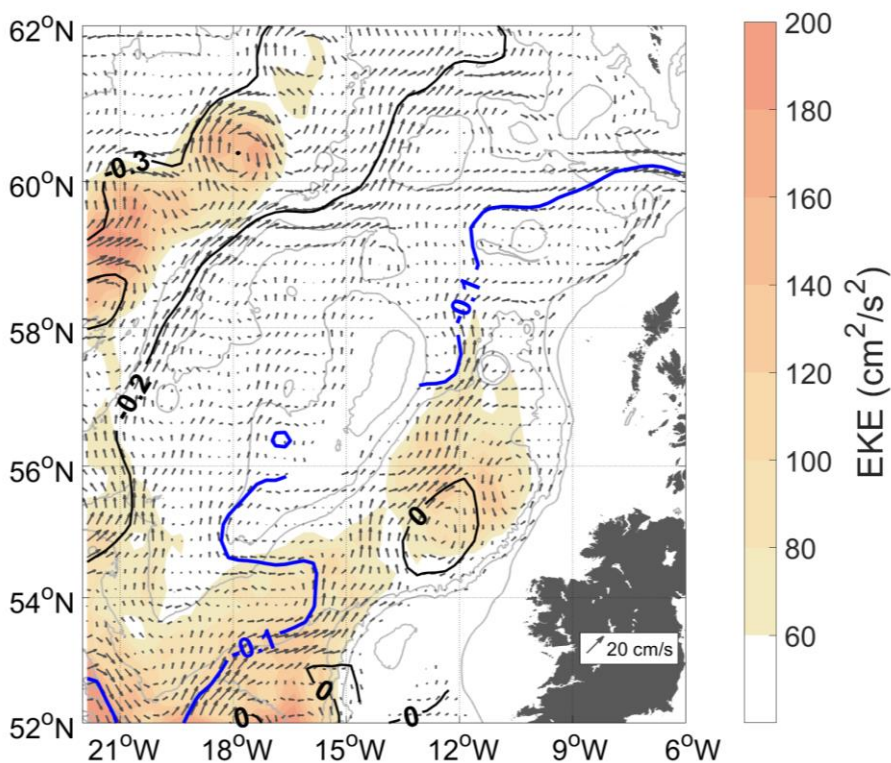
196 |
197

198 **Table S2:** Comparisons of the 4-year mean (standard deviation) of the surface
199 absolute meridional geostrophic current from gridded altimetry with meridional
200 velocity from the mooring array. Meridional currents from the mooring array are
201 computed from the near-surface current meters (100 m depth) at WB1 and EB1,
202 and from the mid-basin geostrophic current calculated at 100 m depth. Mooring
203 and altimetry data are both low-pass filtered with a 25-day window. Units
204 are cm/s.

	WB1	mid-basin	EB1
Mooring	-7.2 (14.5)	3.5 (1.8)	5.5 (10.7)
Altimetry	0.2 (7.6)	4.2 (1.7)	0.9 (8.0)
Difference	-7.4 (6.9)	-0.7 (0.1)	4.6 (2.7)

205
206
207
208
209
210
211

212



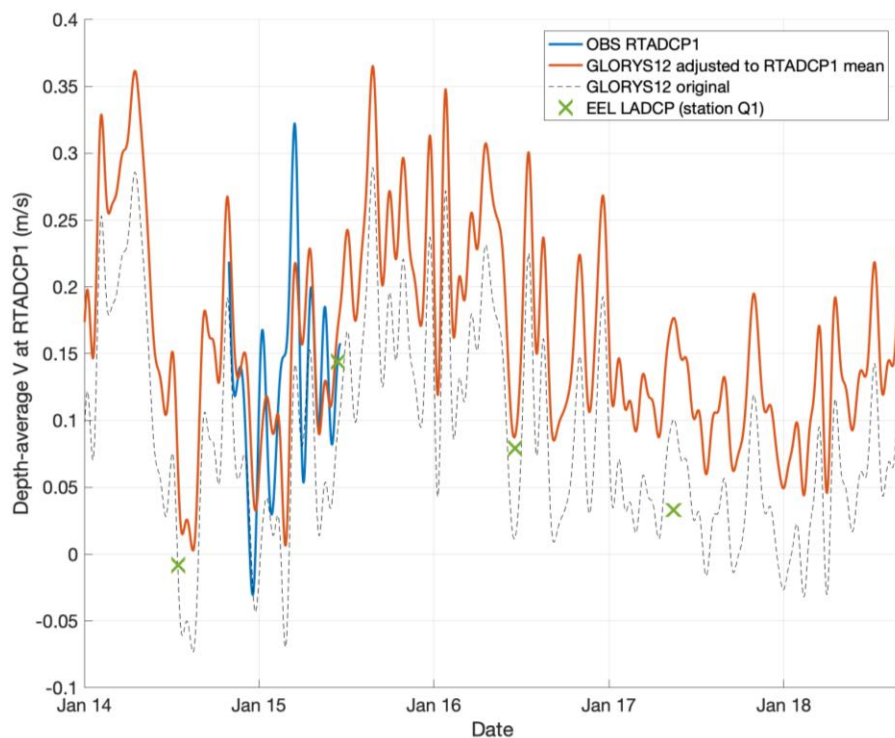
213

214 **Figure S1:** 4-year mean 90-day low-pass filtered EKE (red color scale) and
215 surface absolute geostrophic current (black arrows) calculated during the Jul.
216 2014 – Jul. 2018 period. Data are plotted for water depth deeper than 400 m and
217 velocity superior to 2.5 cm/s . The mean absolute dynamic topography contours
218 are plotted as thick black lines with a contour interval of 0.1 m. Bathymetry
219 contours from ETOPO are shown in grey for the 200, 1000, 2000, and 3000 m
220 contours. Acronyms: eddy kinetic energy (EKE); Earth TOPOgraphic database
221 (ETOPO).

222

223

224
225
226



227

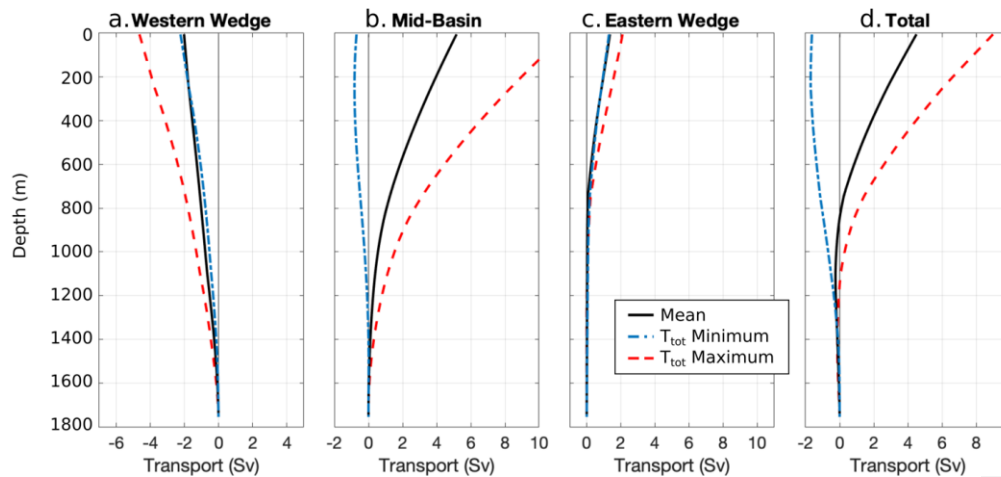
228 **Figure S2:** Depth-average meridional velocity V at the ADCP1 location (57.1°N,
229 9.3°W, water depth of 750m) from 8-months of ADCP observations (blue), from
230 GLORYS12v1 reanalysis (black dashed line), from GLORYS12v1 adjusted to the
231 8-month mean of the ADCP observations (red line), and from LADCP profiles
232 carried out during the Extended Ellett Line cruises (green crosses). The ADCP
233 and GLORYS time-series are 25-day low-pass filtered so their variability reflects
234 similar timescales. The LADCP are de-tided using barotropic tides at the time of
235 each cast, obtained from the Oregon State University Tidal Inversion Software
236 (Egbert & Erofeeva, 2002; <https://www.tpxo.net/>).

237

238

239

240



241

242 **Figure S3:** Cumulative transport integrated from 1760 m to the surface are
243 shown for the western wedge (a), the mid-basin (b), the eastern wedge (c) and
244 the whole section (d). The black solid line corresponds to the 4-year mean. The
245 dashed lines correspond to cumulative transports at the time of the total Rockall
246 Trough transport extrema (the minimum on July 2017 is in blue, the maximum on
247 August 2016 is in red).

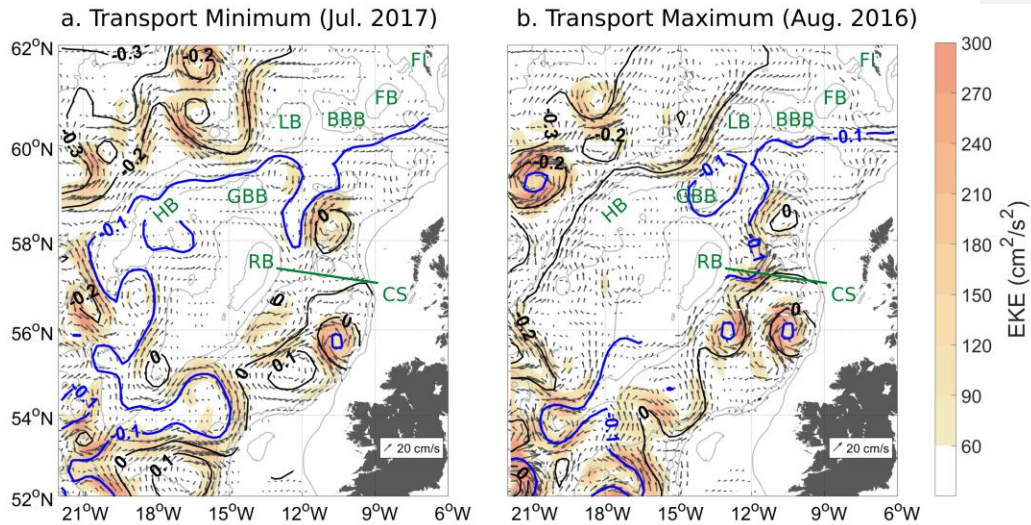
248

249

250

251

252



253

254 **Figure S4:** 90-day low-pass filtered EKE (red color scale) and surface absolute
255 geostrophic current (black arrows) at the time when minimum transport (a) and
256 maximum transport (b) are recorded in the Rockall Trough. The composite states
257 for low and high transport periods are shown on Figure 7. Data are plotted for
258 water depth deeper than 400 m and velocity superior to 2.5 cm/s . The green line
259 along 57.5°N indicates the line along which our mooring array is deployed. The
260 mean absolute dynamic topography contours are plotted as thick black lines with
261 a contour interval of 0.1 m. Bathymetry contours from ETOPO are shown in grey
262 for the 200, 1000, 2000, and 3000 m contours. Acronyms: eddy kinetic energy
263 (EKE); Earth TOPOgraphic database (ETOPO); other acronyms are defined in
264 Figure 1.

265

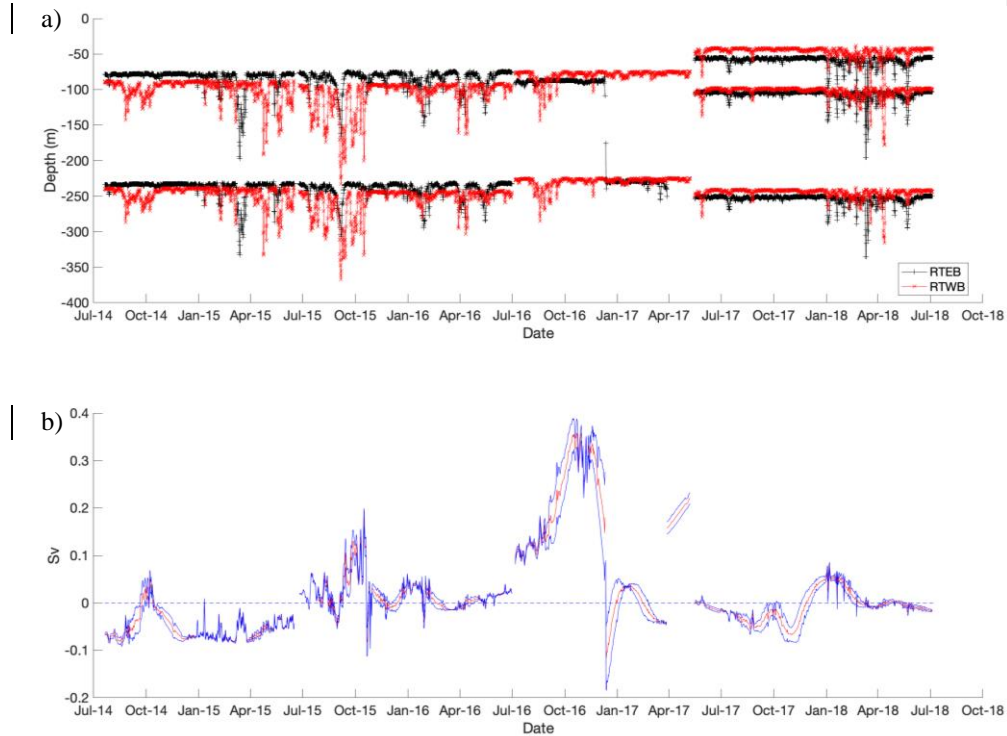
266

267

268

269

270



271

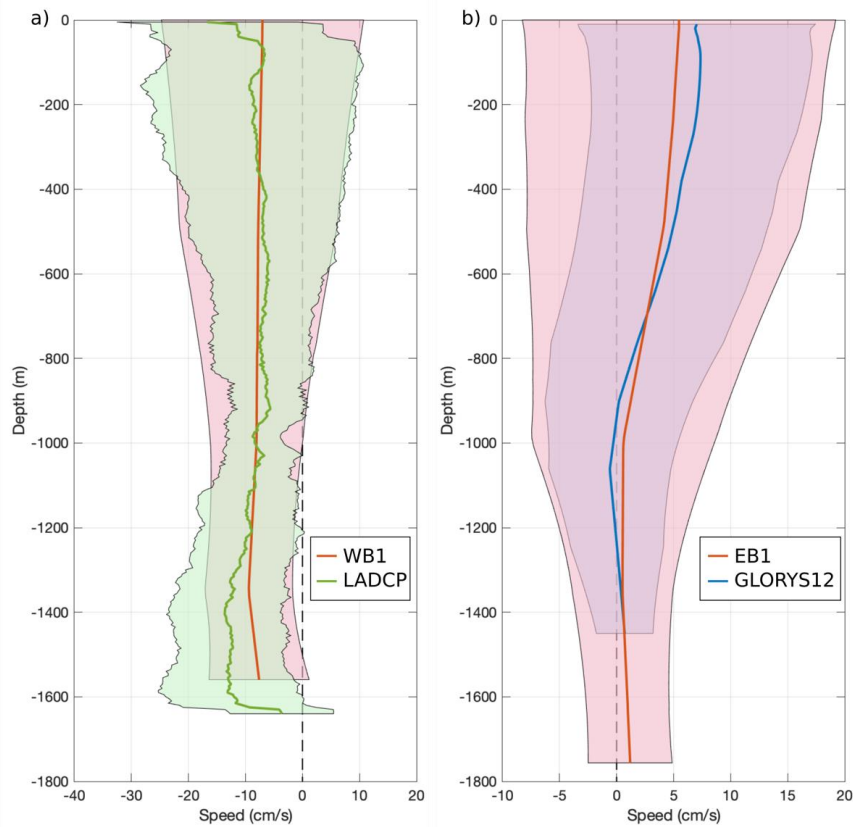
272 **Figure S5:** (a) Time-series of the near-surface pressure from the mooring
273 instruments deployed on EB1 and WB1; (b) Mean bias error (red line) \pm rms
274 error (blue lines) of the transport calculated above 200 m due to the extrapolation
275 of the geostrophic shear from the shallowest instrument depth to the surface.

276

277

278

279

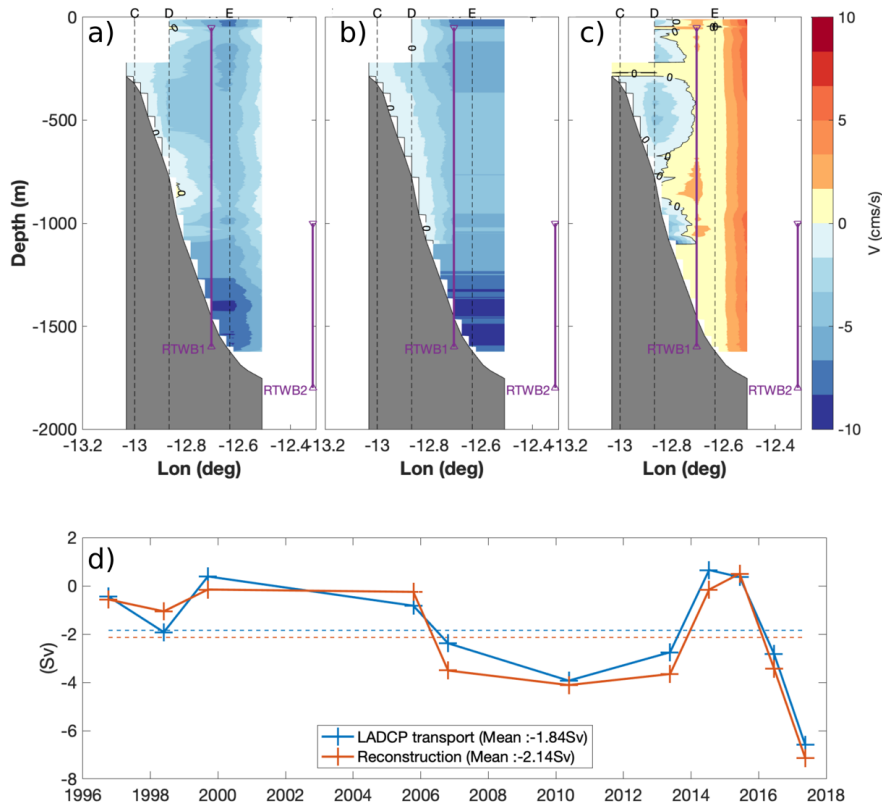


280 **Figure S6:** (a) Mean and standard deviation of the meridional velocity at the
281 WB1 location from 4-years of OSNAP current meters (red line) and LADCP data
282 from 12 EEL summer cruises which took place between 1996 and 2017 (green
283 line); (b) 4-year mean meridional velocity profiles from mooring measurements at
284 the EB1 location (red line) and GLORYS12v1 reanalysis at the same location
285 (blue line). The shaded areas show the mean \pm one standard deviation.

286

287

288



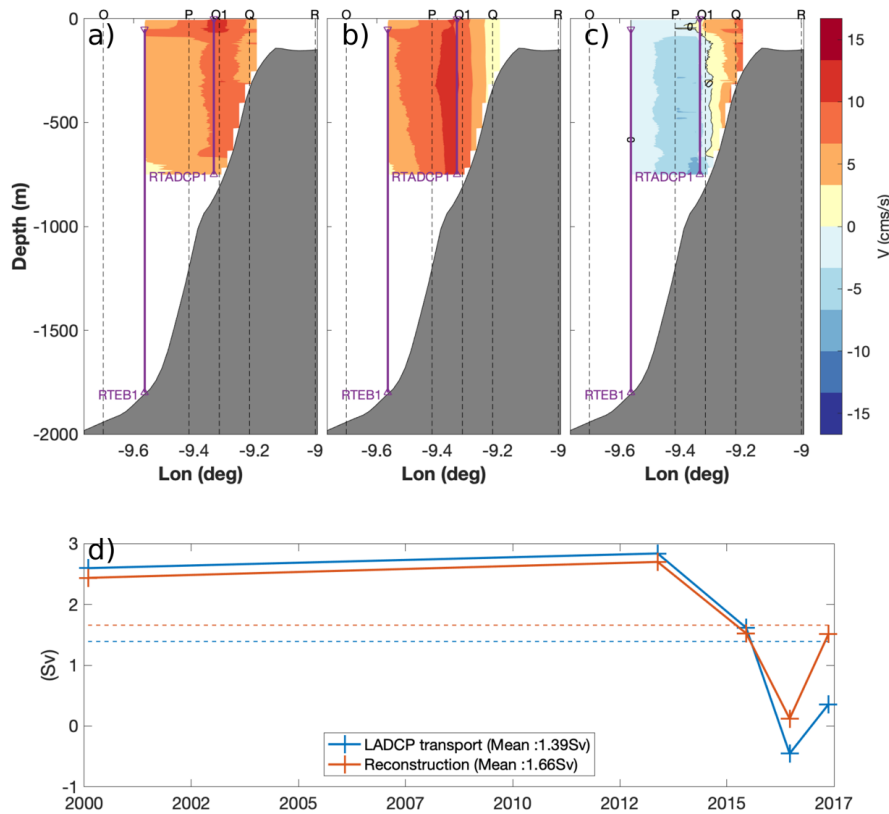
290

291 **Figure S7:** (a) Mean cross-section LADCP velocities over the Western Wedge
 292 area, calculated from the 11 EEL cruises which occupied all stations C, D, E and
 293 F; (b) cross-section velocity reconstructed from the LADCP profiles taken at
 294 station E and extrapolated to the western wedge area following the method
 295 indicated in this article: 1) EEL-LADCP cruises are used to create a profile of
 296 meridional velocity at WB1 location by interpolating the LADCP velocity field; 2)
 297 the western wedge velocity field is created by extending uniformly the WB1
 298 velocities eastward to -12.5 °W, whilst west of WB1, velocities are linearly
 299 interpolated between those at WB1 to zero, either at the eastern boundary of the
 300 wedge (13.0 °W) or the seabed if this was intercepted; 3) the upper 250 m of the
 301 western wedge is filled by linearly interpolating velocities from WB1 to zero at

302 12.9 °W, instead of 13.0 °W in order to exclude from our calculation a northward
303 flow recirculating around Rockall Bank (see the transport calculation section); (c)
304 Mean difference between the LADCP velocities section and the reconstructed
305 Western Wedge velocities; (d) Western Wedge transport calculated from the
306 LADCP velocity profiles of every EEL cruise which occupied stations C, D, E and
307 F (blue line) and from the reconstructed velocity field (red line); the mean (\pm one
308 standard deviation) of the transport differences is 0.30 (\pm 0.62 Sv)

309

310



312

313 **Figure S8:** (a) Mean cross-section LADCP velocities over the upper Eastern
 314 Wedge area (<750m), calculated from the 5 EEL cruises which occupied all
 315 stations O, P, Q1 and Q; (b) cross-section velocity reconstructed following the
 316 method presented in this article: 1) EEL-LADCP cruises are used to create a
 317 profile of meridional velocity at EB1 location by interpolating the LADCP velocity
 318 field; 2) GLORYS12 reanalysis is used to create a profile of meridional velocity at
 319 RTADCP1 location adjusted by + 7.6 cm/s so the 2014-2015 GLORYS mean
 320 velocity at RTADCP1 is the same than the observed one from ADCP1
 321 deployment; 3) The Eastern Wedge velocity field is created by linearly
 322 interpolated the velocity between 9.6W and 9.3W and by linearly decreasing
 323 them to zero at the edge of the continental shelf (9.2 °W); (c) Mean difference

324 between the LADCP velocities section and the reconstructed upper 750 m
325 Eastern Wedge velocities; (d) Eastern Wedge transport calculated from the
326 LADCP velocity profiles of every EEL cruises which occupied station O, P, Q1
327 and Q (blue line) and from the reconstructed velocity field (red line); the mean
328 (\pm one standard deviation) of the transport differences is $-0.27 (\pm 0.58 \text{ Sv})$

329

330

331